J|A|C|S
ARTICLES
Published on Web 08/07/2002

^{13}C NMR Investigation of Solid-State Polymorphism in 10-Deacetyl Baccatin III

James K. Harper, Julio C. Facelli,† Dewey H. Barich, Gary McGeorge,‡ Anna E. Mulgrew, and David M. Grant*

Contribution from the Department of Chemistry, University of Utah, 315 South 1400 East, Salt Lake City, Utah 84112, Center for High Performance Computing, University of Utah, Salt Lake City, Utah 84112 and Bristol-Myers Squibb, 1 Squibb Drive, New Brunswick, New Jersey 08903

Received March 13, 2002. Revised Manuscript Received June 10, 2002

Abstract: To investigate the origins of solid-state NMR shift differences in polymorphs, carbon NMR chemical shift tensors are measured for two forms of solid 10-deacetyl baccatin III: a dimethyl sulfoxide (DMSO) solvate and an unsolvated form. A comparison of ab initio computed tensors that includes and omits the DMSO molecules demonstrates that lattice interactions cannot fully account for the shift differences in the two forms. Instead, conformational differences in the cyclohexenyl, benzoyl, and acetyl moieties are postulated to create the differences observed. X-ray analysis of six baccatin III analogues supports the suggested changes in the cyclohexenyl and benzoyl systems. The close statistical match of the ^{13}C chemical shifts of both polymorphic forms with those calculated using the X-ray geometry of 10-deacetyl baccatin III supports the contention that the B, C, and D rings are fairly rigid. Therefore, the observed tensor differences appear to arise primarily from conformational variations in ring substituents and the cyclohexenyl ring.

Introduction

Molecular conformation in many compounds strongly affects bioactivity. This phenomenon has been extensively examined in proteins, peptides, and smaller bioactive compounds where marked differences in activities are observed for differing stable conformations. In the case of prion proteins, a conformational change is proposed to create an infectious protein (PrP^{Sc}) from a normal cellular protein.[1] In prions, the change is of sufficient significance that the PrP^{Sc} form is proposed to cause Creutzfeldt−Jakob disease, kuru, and Gerstmann−Sträussler syndrome.[2] Work with lipases has further demonstrated that even minor changes in conformation can result in modified bioactivity.[3] Lipases trapped in a range of conformations through a rapid freeze-drying process were retained in solution in the selected conformation by placing the dried lipase into water-restricted environments. Lipase trapped in a near-inactive form reacted preferentially with short-chain (4−8 carbons) triglyceride substrates, while those trapped in conformations closer to the active form were capable of reacting with triglycerides up to 16 carbons long. Such conformational changes are also important in smaller bioactive molecules where investigation often focuses on sets of computer-generated conformational isomers to assess their docking ability with known binding sites.[4]

The investigation of potentially important conformations in both proteins and smaller molecules by computational methods allows a large number of conformations to be rapidly characterized in terms of energy and molecular shape. However, the structures obtained suffer from being theoretical constructs that, at times, fail to accurately reproduce the experimental evidence. The modeling approach is also less useful in cases where the structure of the binding sites is not known. An alternative and complementary approach to conformational investigations involves the preparation and characterization of a variety of solid polymorphs of a given molecule. The distinct lattices of the different forms may differ significantly and can involve the inclusion or omission of solvent molecules. Such studies thus simulate the effect of different environments and provide experimental data regarding energetically favorable conformations of the molecule. X-ray diffraction analyses of such polymorphs are often infeasible due to the inability to grow suitable crystals of all lattice forms. However, solid-state NMR is capable of analyzing such materials even when the resulting solid includes a mixture of several lattice types[5] or consists of amorphous material.[6] Solid-state NMR thus provides a complementary technique for the characterization of polymorphic solids.

In the work described here, ^{13}C solid-state NMR is used to characterize two polymorphs of 10-deacetyl baccatin III (Figure 1), a molecule containing 29 carbons that forms the major portion of the anticancer drug paclitaxel (Taxol). These polymorphs include a dimethyl sulfoxide (DMSO) solvate previously described by X-ray crystallography[7] and a second solid forming

* Address correspondence to this author. E-mail: grant@chemistry.utah.edu.
† Center for High Performance Computing, University of Utah.
‡ Bristol-Myers Squibb.

(1) Baldwin, M. A.; James, T. L.; Cohen, F. E.; Prusiner, S. B. *Biochem. Soc. Trans.* **1998**, *26*, 481.
(2) (a) Gajdusek, D. C. *Science* **1977**, *197*, 943. (b) Masters, C. L.; Gajdusek, D. C.; Gibbs, C. J., Jr. *Brain* **1981**, *104*, 535.
(3) González-Navarro, H.; Bañó, M. C.; Abad, C. *Biochemistry* **2001**, *40*, 3174.
(4) Lambert, M. H. In *Practical Applications of Computer-Aided Drug Design*; Charifson, P. S., Ed.; Marcel Dekker: New York, 1997; pp 243−303.
(5) Harper, J. K.; Grant, D. M. *J. Am. Chem. Soc.* **2000**, *122*, 3708.
(6) (a) Schmidt-Rohr, K.; Spiess, H. W. *Multidimensional Solid-State NMR and Polymers*; Academic Press: San Diago, 1994; Chapter 5. (b) Orendt, A. O.; Solumn, M. S.; Sethi, N. K.; Pugmire, R. J.; Grant, D. M. In *Advances in Coal Spectroscopy*; Meuzelaar, H. L. C., Ed.; Plenum Press: New York, 1992; pp 215−254.

Table 1. Principal Values for Polymorph I of 10-Deacetyl Baccatin III DMSO Solvate

		isotropic		principal values, experimental (theoretical)		
carbon no.	carbon type[a]	FIREMAT[b]	solution	11	22	33
1[c]	Q	78.7	77.0	93.1 (92.0)	83.6 (82.0)	59.3 (58.9)
2	CH	77.4	74.9	111.2 (115.4)	73.1 (76.4)	48.0 (50.2)
3	CH	47.7	46.6	59.9 (61.4)	44.3 (40.2)	39.1 (39.1)
4	Q	80.9	80.1	96.3 (95.9)	89.9 (93.4)	56.4 (55.0)
5	CH	84.4	83.8	108.5 (105.0)	98.8 (95.2)	45.9 (43.1)
6	CH_2	37.6	36.6	59.8 (58.3)	40.3 (34.4)	12.7 (12.5)
7[d]	CH	70.8	71.0	91.9 (87.1)	73.3 (77.8)	47.2 (44.8)
8	Q	58.8	57.1	79.4 (84.0)	52.0 (57.7)	45.0 (48.2)
9	Q	216.1	210.4	291.7 (299.2)	268.0 (261.2)	88.7 (90.2)
10	CH	75.0	74.4	97.3 (92.1)	71.4 (76.0)	56.2 (54.5)
11	Q	135.5	134.5	231.6 (234.7)	135.1 (152.9)	39.8 (38.4)
12	Q	141.5	141.6	238.2 (237.3)	144.7 (154.9)	41.7 (47.5)
13[d]	CH	68.2	66.1	89.5 (91.3)	75.4 (73.4)	39.8 (41.2)
14[e]	CH_2	41.2	39.2[e]	65.1 (72.0)	43.1 (48.0)	15.4 (12.6)
15	Q	43.7	42.5	52.8 (53.2)	44.2 (46.9)	34.1 (41.1)
16	CH_3	29.4	26.8	48.8 (46.3)	32.9 (34.9)	6.5 (3.0)
17	CH_3	21.3	20.2	36.6 (35.0)	22.5 (23.2)	4.9 (5.6)
18	CH_3	15.5	14.8	26.4 (29.1)	15.2 (18.1)	5.0 (3.5)
19	CH_3	11.1	9.7	17.6 (20.3)	11.3 (14.5)	4.5 (4.9)
20[c]	CH_2	78.7	75.5	99.7 (96.1)	95.1 (94.9)	41.1 (38.4)
21[f]	Q	167.9	165.3	255.4 (254.2)	134.9 (130.2)	113.5 (114.0)
22	Q	131.0	130.3	221.3 (214.4)	138.6 (145.5)	33.2 (21.5)
25[g]	CH	133.4	129.5	234.0 (230.3)	148.0 (148.2)	18.2 (10.0)
28[f]	Q	172.5	169.6	264.8 (256.5)	140.5 (134.3)	112.1 (115.4)
29	CH_3	26.2	22.3	44.9 (39.9)	34.3 (29.0)	−0.5 (−6.8)

[a] Determined by spectral editing analyses. [b] Determined by averaging the three FIREMAT principal values. [c] These isotropically degenerate peaks were proven to be the expected carbon types through a spectral editing analysis. [d] Shift assignments shown are interchangeable. [e] The solution isotropic signal for this carbon was obscured by the overlapping DMSO signal, and thus an accurate shift value was not obtained. This signal in the solid state is also isotropically degenerate with a DMSO signal, but the tensor fitting picks out the C14 values as a result of line width differences. A second DMSO line of 3 carbon intensity was also found at approximately 38 ppm. [f] Shift assignments shown are interchangeable. [g] This peak was assigned as C25 based on the near invariance of C22 with temperature, consistent with motion about an axis bisecting C22 and C25. This motion would influence C23, C24, C26, and C27 but leave C25 relatively stationary. Accordingly, resonances from C23, C24, C26, and C27 are absent from the room-temperature spectrum.

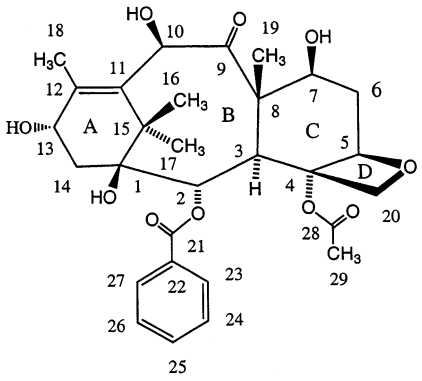

Figure 1. Structure of 10-deacetyl baccatin III showing the numbering used and the A, B, C, and D ring designations.

a well-defined lattice but having no crystals suitable for X-ray analysis. Carbon chemical shift tensor principal values are obtained for both forms using the FIREMAT technique.[8] Measuring ^{13}C shift tensors in molecules containing more than a few carbons has only recently become routinely available and has been demonstrated to be quite sensitive to molecular conformation. The ^{13}C tensor data on the two distinct forms of 10-deacetyl baccatin III suggest conformational differences. The influence of environment on tensors is investigated by computing ab initio tensors with and without DMSO molecules present to demonstrate that intermolecular lattice factors are unlikely to produce the observed differences. X-ray diffraction dihedral angle data on baccatin III analogues are then used to clarify the structural origins of the observed differences. The ^{13}C NMR shift tensor data suggest that the largest conformational differences between polymorphs arise from changes external to the tetracyclic moiety and that the majority of the ring system is fairly rigid.

Results and Discussion.

^{13}C Tensor Measurements and Shift Assignments. The NMR chemical shift tensor contains six measurable shift values per magnetically inequivalent nucleus. Typically, solid samples are required to measure these tensor components and all six tensor values are usually observable only in single-crystal samples. In microcrystalline powders (i.e., those consisting of a well-defined lattice but lacking large single crystals), only the three principal components of the shift tensor can be routinely observed, and these principal values are reported in this work.

In 10-deacetyl baccatin III, two different solids were obtained and analyzed (as described in the Experimental Section), a highly crystalline form containing DMSO solvent molecules and a second form with no included solvent. Herein, the two polymorphs are referred to as forms I and II for the DMSO solvate and the second form, respectively. Both forms represent well-defined lattices, as indicated by narrow ^{13}C isotropic NMR line shapes. The presence of only one isotropic line per carbon further indicates the presence of only one molecule per crystallographic asymmetric unit. Principal values for most carbons of the two polymorphic forms were measured using the FIREMAT technique, and all principal values are reported in Tables 1 and 2. The aliphatic region of the FIREMAT

(7) Harper, J. K.; Dalley, N. K.; Mulgrew, A. E.; West, F. G.; Grant, D. M. *Acta Crystallogr.* **2001**, *C57*, 64.
(8) Alderman, D. W.; McGeorge, G.; Hu, J. Z.; Pugmire, R. J.; Grant, D. M. *Mol. Phys.* **1998**, *95*, 1113.

Table 2. Principal Values for Polymorph II of 10-Deacetyl Baccatin III

	isotropic		principal values, experimental (theoretical)[a]		
carbon no.	FIREMAT[b]	solution	11	22	33
1	77.7	77.0	91.7 (94.2)	85.6 (85.4)	55.8 (56.8)
2	74.0	74.9	107.4 (108.6)	65.0 (71.1)	49.7 (46.8)
3	47.3	46.6	56.2 (59.7)	49.2 (40.3)	36.6 (38.9)
4	81.5	80.1	96.7 (101.6)	92.6 (98.1)	55.3 (58.1)
5	83.7	83.8	106.7 (104.2)	98.9 (95.1)	45.4 (44.3)
6	37.9	36.6	59.6 (58.7)	39.7 (36.1)	14.3 (14.2)
7	72.3	71.0	93.0 (86.8)	75.3 (82.6)	48.6 (44.7)
8	58.8	57.1	78.3 (72.2)	51.4 (57.7)	46.6 (48.1)
9	212.6	210.4	290.3 (301.0)	258.7 (233.5)	88.8 (94.6)
10	76.6	74.4	98.6 (91.8)	72.4 (76.9)	58.8 (50.5)
11	132.9	134.5	229.9 (239.5)	128.4 (154.6)	40.3 (36.1)
12	148.5	141.6	245.9 (236.9)	154.9 (147.9)	44.7 (44.4)
13	66.8	66.1	94.1 (95.4)	68.3 (72.9)	37.9 (39.7)
14	39.5	39.2[c]	65.6 (61.9)	45.1 (46.9)	7.9 (11.1)
15	43.7	42.5	52.7 (53.5)	44.4 (46.8)	34.0 (41.9)
16	26.8	26.8	46.9 (46.0)	33.5 (30.5)	0.0 (−1.3)
17	19.8	20.2	36.1 (34.8)	19.0 (22.5)	4.3 (5.9)
18	16.4	14.8	28.7 (27.7)	14.4 (15.2)	6.0 (1.8)
19	11.5	9.7	20.0 (18.9)	12.3 (13.5)	2.2 (4.2)
20	76.2	75.5	99.2 (97.1)	90.0 (91.0)	39.5 (35.3)
21	165.8	165.3	255.2 (266.3)	130.6 (130.2)	111.5 (120.8)
22[d]	128.0	130.3	219.8 (214.4)	138.9 (141.9)	25.3 (23.0)
23[e]	130.4	129.5	228.5 (225.4)	150.8 (152.3)	11.8 (9.3)
24[e]	129.5	129.5	223.7 (229.3)	156.1 (134.7)	8.6 (9.7)
25[e]	128.9	128.7	227.8 (234.7)	146.9 (144.1)	12.0 (9.3)
26[e]	133.7	133.2	236.9 (228.2)	153.8 (138.1)	10.5 (9.6)
28	173.4	169.6	264.4 (274.0)	147.2 (147.4)	108.5 (119.6)
29	22.6	22.3	38.3 (38.4)	31.0 (31.7)	−1.5 (−7.7)

[a] Assignments were made by comparison to polymorph I. [b] Determined by averaging the three FIREMAT principal values. [c] The solution isotropic signal for this carbon was obscured by the overlapping DMSO signal, and thus an accurate shift value was not obtained. [d] INADEQUATE connections in the benzoyl ring were not established, and the order shown for solution isotropic shifts of C's 22−26 is interchangeable. [e] Solid-state assignments shown are interchangeable.

spectrum of polymorph II is illustrated in Figure 2. Shift values for four carbons in form I (tentatively assigned as C23, C24, C26, and C27) are unobserved due to molecular motion in the solid and are thus omitted from Table 1.

Before physical phenomena can be correlated with shifts, accurate assignments to molecular positions must be made. For polymorph I, all chemical shift assignments were made by first assigning a carbon type (i.e., CH_3, CH_2, CH, or quaternary) to each line by a spectral editing procedure.[9] Final assignments were then provided using a previously described procedure involving comparison of experimental principal values with ab initio computed shifts from the X-ray geometry (Table 1).[10] Differences in experimental principal values for the distinct molecular positions were larger than the error in computed tensors ($\sigma = 4.72$ ppm) in most cases, allowing confident assignment (>80% probability) of shifts. In form I, assignment ambiguities remain between C7 and C13 and, separately, between C21 and C28 that cannot be resolved at the present level of computation. For polymorph II, the tensor shifts were sufficiently similar to those of form I that assignments were made by analogy (Table 2). Solution shifts are also included in Tables 1 and 2 for comparison and show that these differ from the solid isotropic shifts by an average of 2.2 ppm for form I and by 2.0 ppm in solid II. Both lattice types have several isotropic shifts differing significantly from solution values with changes as large as 6.9 ppm observed. Three changes in relative isotropic peak ordering are observed between the solution shifts and lattice II with carbons 2 and 20, respectively, occurring before carbon 10 in the solid but with a relative ordering of C10, C2, and C20 in solution. This change in relative ordering emphasizes the risks of using solution shifts to assign solid spectra.

Table 3. Differences in Experimental Tensor Shifts in Polymorphs I and II (I Minus II)[a]

position	$\Delta\delta_{11}$	$\Delta\delta_{22}$	$\Delta\delta_{33}$
1	1.4	−2.0	3.5
2	3.8	**8.1**	−1.7
3	3.7	−4.9	2.5
4	−0.4	−2.7	1.1
5	1.8	−0.1	0.5
6	0.2	0.6	−1.6
7	−1.1	−2.0	−1.4
8	1.1	0.6	−1.6
9	1.4	**9.3**	−0.1
10	−1.3	−1.0	−2.6
11	1.7	**6.7**	−0.5
12	**−7.7**	**−10.2**	−3.0
13	−4.6	**7.1**	1.9
14	−0.5	−2.0	**7.5**
15	0.1	−0.2	0.1
16	1.9	−0.6	**6.5**
17	0.5	3.5	0.6
18	−2.3	0.8	−1.0
19	−2.4	−1.0	2.3
20	0.5	**5.1**	1.6
21	0.2	4.3	2.0
22	1.5	−0.3	**7.9**
28	0.4	**−6.7**	3.6
29	**6.6**	3.3	1.0

[a] Bold values denote differences that are significantly larger than the error in computed tensors.

Lattice or Conformation? Origin of Shift Differences in Polymorphs. Several differences in principle values are observed between the two polymorphs of 10-deacetyl baccatin III at corresponding molecular positions (see Table 3). Differences of less than approximately 1.0 ppm are considered within the experimental error of the measurement, but significantly larger ones may arise from either intermolecular lattice differences or conformational differences. Previous ^{13}C tensor work on molecules of moderate polarity has demonstrated that very accurate tensors may be computed using the isolated molecule if the correct geometry (i.e., X-ray positions for non-hydrogen atoms) is used.[11,10b] Such ^{13}C computed tensors have proven capable of modeling even the minor geometric differences found in the different molecules of the asymmetric unit.[10b,12] This ability to obtain accurate ^{13}C shifts while omitting lattice features argues that tensor differences for differing geometries arise primarily from conformational differences rather than lattice differences. However, in charged compounds and some polar structures inclusion of lattice perturbations has been demonstrated to be important.[13] 10-Deacetyl baccatin III contains both

(9) Hu, J. Z.; Harper, J. K.; Taylor, C.; Pugmire, R. J.; Grant, D. M. *J. Magn. Reson.* **2000**, *142*, 326.
(10) (a) Harper, J. K.; Mulgrew, A. E.; Li, J. Y.; Barich, D. H.; Strobel, G.; Grant, D. M. *J. Am. Chem. Soc.* **2001**, *123*, 9837. (b) Harper, J. K.; McGeorge, G.; Grant, D. M. *J. Am. Chem. Soc.* **1999**, *121*, 6488.
(11) Harper, J. K.; McGeorge, G.; Grant, D. M. *Magn. Reson. Chem.* **1998**, *36*, S135.
(12) (a) Szelejewska-Wozniakowska, A.; Chilmonczyk, Z.; Les, A.; Wawere, I. *Solid State Nucl. Magn. Reson.* **1998**, *13*, 63. (b) Maciejewska, D.; Herold, F.; Wolska, I. *J. Mol. Struct.* **2000**, *553*, 73.
(13) (a) Stueber, D.; Guenneau, F. N.; Grant, D. M. *J. Chem. Phys.* **2001**, *114*, 9236. (b) deDios, A. C.; Oldfield, E. *Chem. Phys. Lett.* **1993**, *205*, 108. (c) deDios, A. C.; Laws, D. D.; Oldfield, E. *J. Am. Chem. Soc.* **1994**, *116*, 7784.

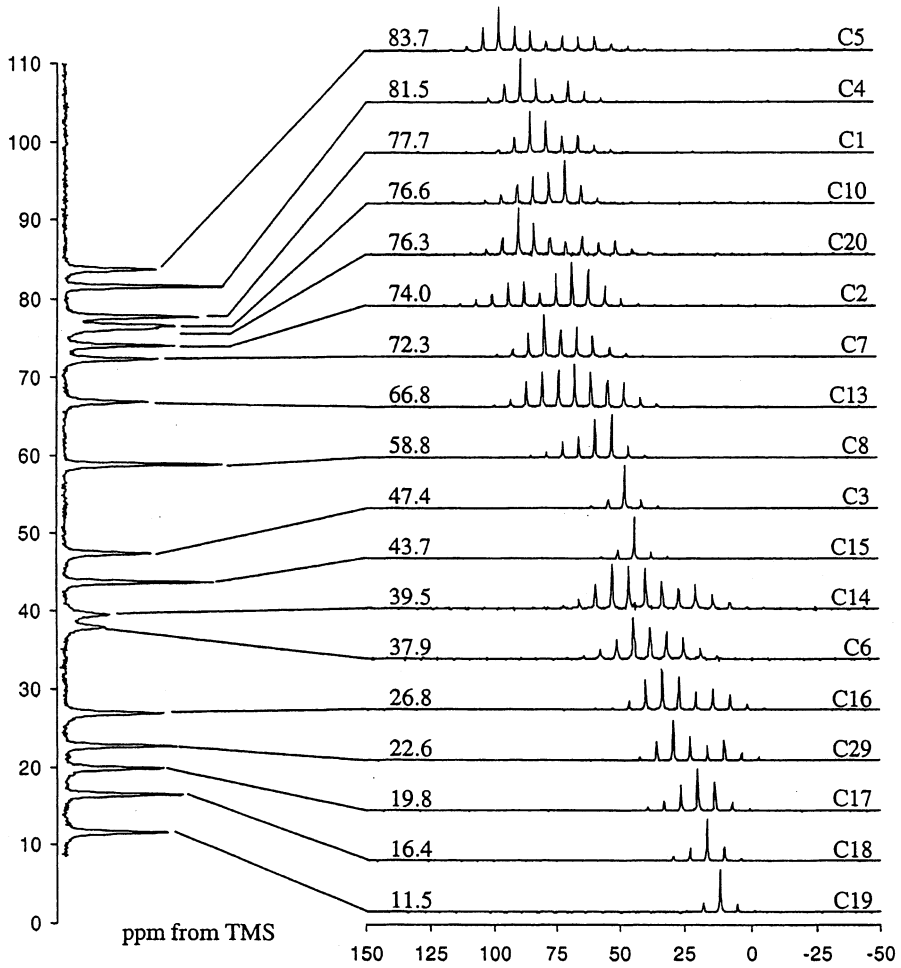

Figure 2. The FIREMAT spectrum for the aliphatic region of polymorph II of 10-deacetyl baccatin III. The spectrum displays isotropic shifts for each carbon on the left side of the figure and the corresponding tensor patterns with assignments to the right.

polar and nonpolar portions, making it unclear to what extent lattice influences tensor shifts. Fortunately, the influence of lattice can be investigated by computing tensors both with and without the DMSO molecules present in form I. Such computations demonstrate that the DMSO molecules have only a minor influence on tensors. Specifically, inclusion of the two DMSO molecules changes only three tensor values by more than 3 ppm (i.e., the δ_{22} component of C9 by 6.81 ppm, the δ_{22} component of C14 by 3.89 ppm, and the δ_{33} value of C16 by 5.97 ppm). In contrast, large experimental tensor differences (>6.0 ppm) between polymorphs are observed at carbons 2, 9, 11, 12, 13, 14, 16, 22, 28, and 29 as summarized in Table 3, indicating that lattice interactions account for differences in only 3 of the 10 differing carbons. The failure of DMSO to significantly influence shifts supports previous contentions[5,10b] that conformational differences between the polymorphs give rise to the majority of the observed differences.

Conformational Origins of Tensor Differences in Polymorphs. Variations in tensors in the two polymorphs of 10-deacetyl baccatin III are most evident in the cyclohexenyl ring with large differences observed at C11, C12, C13, and C14. Previous work on the closely related allyl alcohol, verbenol (Figure 3), suggests that the origin of these differences may be a difference in the C13 hydroxy dihedral angle. In verbenol, tensor shifts in an analogous cyclohexene ring (at C2, C3, C4, and C5) were demonstrated to strongly depend on the orientation

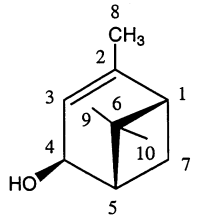

Figure 3. Structure of verbenol.

of the hydroxy hydrogen with changes as large as 12 ppm in principal values predicted to arise from differing orientations of the hydroxy hydrogen.[5] In 10-deacetyl baccatin III, a second allylic hydroxy is also present at C10. However, this hydroxy is unlikely to be the origin of the observed differences between the polymorphs as the C10 tensors in both forms are nearly identical, indicating very similar conformations. Likewise, the similarity of the principal values at C1 makes hydroxy hydrogen variation here an improbable source of the differences observed.

Additional tensor changes at C22 (in the δ_{33} component) also likely arise from differences in conformations in the benzoyl moiety resulting from molecular motion. In form I, the benzoyl ring experiences motion on the NMR time scale as shown by the low-temperature analysis (Figure 4). At room temperature, this motion causes aromatic carbons near 130 ppm to be missing from the spectrum. The presence of the C21 signal at room temperature in both forms implies rigidity at this position and

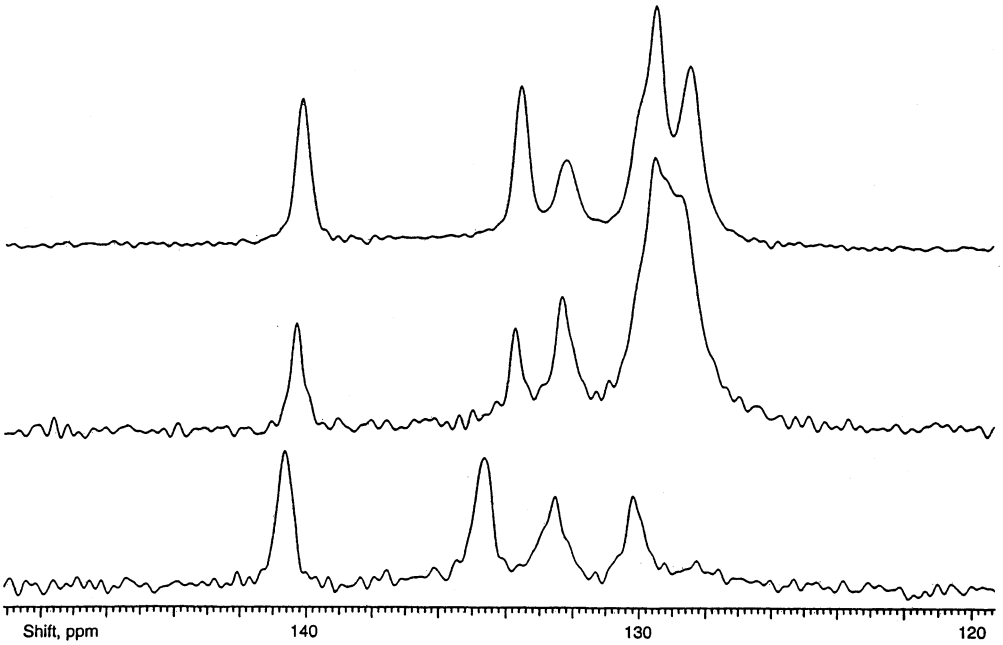

Figure 4. Low-temperature isotropic spectra of the aromatic region of 10-deacetyl baccatin III DMSO solvate. A limited temperature range of 23, −100, and −120 °C was collected (bottom to top, respectively) to qualitatively illustrate the presence of molecular motion in the benzoyl moiety. In the room-temperature FIREMAT analysis, signals for four carbons are missing due to this motion. The 23 °C spectrum exhibits minor shift differences relative to values listed in Table 1 that are assumed to arise from differences in referencing.

suggests that the motion involves changes in the relative orientations of the C═O and benzene moieties. Evidence supporting this hypothesis is found in the X-ray analysis of docetaxel (Taxotere) where the C2-benzoyl is found to deviate significantly from coplanarity with the benzene moiety.[14] Such changes in the relative orientations reduce the π-overlap between the carboxyl and benzene moieties, causing a lengthening of the C21−C22 bond. This increased bond length should be reflected in the δ_{22} and δ_{33} components of C22. Similar changes are also expected in C21 in the δ_{22} and δ_{33} values. The observation of such changes argues that a motionally induced deviation from coplanarity is the origin of the tensor differences at C22. The near invariance of all nonaromatic signals in the variable-temperature spectra further suggests that the motion present primarily involves the benzoyl moiety. The variation at C29 thus appears to arise from a different origin and may be explained in terms of steric factors.

Methyl tensors have been suggested as sensitive indicators of steric strain on the methyl hydrogens.[10b] In 10-deacetyl baccatin III, a rotation of the C4 acetyl group about the C28−O bond could bring the C29 methyl hydrogens into proximity of the C20 methylene hydrogens, resulting in a change in the C29 methyl tensor. Previous analyses predict that such an interaction would cause the δ_{11} or δ_{22} components to move to lower frequencies. The observation of such a change in the δ_{11} component of form II supports this hypothesis. This scenario also requires the tensor of C20 to change. The δ_{22} component of form II is indeed found to move to a lower frequency, providing further support for this hypothesis. Here, the suggested origins for all observed differences involve conformational change in substituents of the tetracyclic moiety rather than changes in the rings themselves. An alternative explanation would be variation in the ring system conformations. X-ray structures of baccatin III analogues provide independent data to investigate the proposed rigidity of the tetracyclic ring system.

X-ray Structures of Analogues of 10-Deacetyl Baccatin III and Implications for Polymorphs. Six baccatin III analogues, previously described by X-ray analysis, contain the common structural fragment shown in Figure 5 and allow investigation of structural variation in the tetracyclic moiety. The chosen structures include baccatin III,[15] 10-deacetyl baccatin III,[7] and the baccatin III moiety excised from paclitaxel,[16] docetaxel,[13] 2-carbamate taxol,[17] and 7-mesyltaxol.[18] Paclitaxel contains two molecules per asymmetric unit and thus provides two baccatin III moieties for analysis, providing a total of seven structures available for comparison. These compounds contain a diversity of substituents external to the ring and thus offer a broad view of flexibility in the tetracyclic ring system. All dihedral angles in the four rings were compared for the seven structures, revealing five dihedral angles differing by nearly 10° (Table 4). Interestingly, the observed differences occur primarily in the cyclohexenyl moiety, suggesting ring variation as a potential contributor to tensor variation in this moiety along with the C13 hydroxy variation previously described. Overall, these geometrical differences in baccatin III analogues support the conclusion that the tetracyclic ring system is quite rigid with the notable exception of the cyclohexenyl ring. For the cyclohexenyl ring carbons, additional calculations are needed to account for shift changes due to variations in both ring geometry and hydroxy dihedral angle.

The large changes observed in the shifts of the cyclohexenyl (or A ring) carbons can be attributed to either one or both of two different mechanisms: (i) a direct effect on the chemical shifts due to changes in the orientation of the OH group; (ii) an

(14) Gueritte-Voegelein, F.; Guenard, D.; Mangatal, L.; Potier, P.; Guilhem, J.; Cesario, M.; Pascal, C. *Acta Crystallogr.* **1990**, *C46*, 781.

(15) Gabetta, B.; Bellis, P. D.; Pace, R. *J. Nat. Prod.* **1995**, *58*, 1508.
(16) Mastropaolo, D.; Camerman, A.; Luo, Y.; Brayer, G. D.; Camerman, N. *Proc. Natl. Acad. Sci. U.S.A.* **1995**, *92*, 6920.
(17) Gao, Q.; Golik, J. *Acta Crystallogr.* **1995**, *C51*, 295.
(18) Gao, Q.; Chen, S.-H. *Tetrahedron Lett.* **1996**, *37*, 3425.

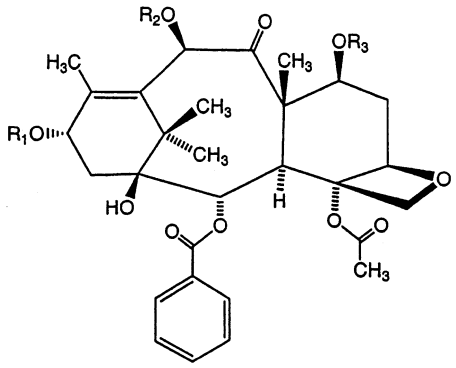

	R_1	R_2	R_3
10-Deacetyl baccatin III	H	H	H
Baccatin III	H	Acetyl	H
Paclitaxel	-C(O)-CH(OH)-CH(Ph)-NH-C(O)-Ph	Acetyl	H
Docetaxel	-C(O)-CH(OH)-CH(Ph)-NH-C(O)-t-butyl	Acetyl	H
7-mesylpaclitaxel	-C(O)-CH(OH)-CH(Ph)-NH-C(O)-Ph	Acetyl	SO_2CH_3
2'-carbamate taxol	-C(O)-CH(O-C(O)-NH_2)-CH(Ph)-NH-C(O)-Ph	Acetyl	H

Figure 5. X-ray-characterized baccatin III analogues. The diverse range of substituents provides a broad view of structural diversity in the A, B, C, and D rings of the baccatin III moiety.

indirect effect on the chemical shift due to geometric changes in the cyclohexenyl ring induced by changes in the orientation of the OH group. Note that the results discussed above on the flexibility of the cyclohexenyl ring preclude the a priori elimination of the second mechanism. To differentiate between contributions to ^{13}C tensor variations in the A ring from these mechanisms, two sets of calculations were performed on verbenol involving C5−C4−O−H dihedral angle variation. In the first set, the hydroxy was rotated about the C−O axis in 30° increments, the angle fixed and tensors computed without energy minimization of the remaining structure. The remaining geometry was placed in the minimum energy geometry as determined from previous work.[5] These calculations provide an estimate of the direct effect of the rotation of the OH on the ^{13}C chemical shifts. A second set of calculations used structures with the same C5−C4−O−H angles of the first set but included energy minimization of all other structural parameters at each angle before tensor calculation. These calculations provide an estimate of the combined effects of OH rotation and ring geometry induced changes of the chemical shift. The differences in the two values at any given point give approximate tensor variation from changes in ring geometry alone.

A comparison of these data shows that the contribution of the direct effect varies with the C5−C4−O−H dihedral angle. In some regions, nearly all of the observed tensor variation arises directly from hydroxy rotation, while other angles reflect significant contributions from changes in ring geometry. This is illustrated in Figure 6 where the direct and indirect contributions are shown for the δ_{11}-component of C4. Similar data are observed for carbons 2, 3, and 5 but are not included here. The observed carbon tensors therefore result from both a hydroxy orientation and a corresponding best geometry for the cyclohexenyl ring. Analysis of the data for carbons 2, 3, 4, and 5 combined shows that, overall, each factor contributes approximately equally to the variation. These data suggest that the geometry and hydroxy hydrogen orientation of the cyclohexyl ring of 10-deacetyl baccatin III may be found by varying the C12−C13−O−H angle, fixing the selected angle, performing an energy minimization, and computing a corresponding tensor. A comparison with experimental tensors would then allow selection of a best structure. Presently, such an investigation has not been performed due to the computational cost arising from the evaluation of multiple structures containing the 39 heavy atoms of 10-deacetyl baccatin III.

Probable Structures for Polymorph II. Despite computational challenges, potential structures of polymorph II may still be described. Tensors for two geometries of 10-deacetyl baccatin III have been computed, the X-ray geometry and an energy-minimized structure. A comparison of these computed tensors to experimental values for polymorph II shows that tensors from the X-ray geometry fit significantly better than those from the optimized geometry as determined by an *F*-test. In fact, when all tensors are considered together, polymorphs I and II fit the X-ray data with statistically indistinguishable quality. This result supports the contention that forms I and II differ only in orientation of a few substituents and not significantly in overall geometry. These data also illustrate the potential for error in structures obtained from energy calculations alone and demonstrate the contribution that tensor data may make in such structural refinements. These tensor data considered together with X-ray structures of baccatin III analogues suggest that polymorph II differs in the C13 hydroxy hydrogen orientation and in the geometry of the cyclohexenyl ring. There appear to also be differences in the benzoyl moiety at C2 and the acetyl moiety at C4. Other differences in the ring systems appear to be rather minor and suggest that studies of larger systems containing baccatin III moieties (e.g., paclitaxel and docetaxel) may assume a "typical structure" for the baccatin III region without introducing significant errors.

Conclusions

Solid-state NMR tensors have been obtained for two polymorphic structures of 10-deacetyl baccatin III and demonstrate that structural variations occur primarily in the ring substituents and the cyclohexenyl ring. These NMR data, coupled with X-ray data of baccatin III analogues, suggest that the B, C, and D rings are fairly rigid. Tensors thus provide the information needed to infer structure in unknown polymorphs from a known form. The sensitivity of shift tensors to even the minor conformational variations of 10-deacetyl baccatin III portends a greater usefulness of this approach in the characterization of conformationally varied polymorphs. These data on 10-deacetyl baccatin III provide the necessary foundation for more extensive solid-state NMR studies of other bioactive taxanes. Recent work has demonstrated that solid-state NMR analyses can significantly contribute to structural analyses of paclitaxel bound to the protein tubulin.[19] Chemical shift tensors may allow further refinement of this complex and offer a general method for examining complexes with other taxanes such as docetaxel.

Experimental Section

Solid 10-deacetyl baccatin III DMSO solvate was prepared by evaporating a DMSO solution of 10-deacetyl baccatin III under vacuum (200 mmHg). This approach resulted in several large crystals that were ground to a powder for evaluation by NMR. The second solid-state form of 10-deacetyl baccatin III was obtained as a gift from Bristol-Myers Squibb and was analyzed as received.

(19) Yankun, L.; Poliks, B.; Cegelski, L.; Poliks, M.; Gryczynski, Z.; Piszczek, G.; Jagtap, P. G.; Studelska, D. R.; Kingston, D. G. I.; Schaefer, J.; Bane, S. *Biochemistry* **2000**, *39*, 281.

Table 4. Large Differences in the X-ray Dihedral Angles of the Baccatin III Moiety of Analogues

	compound[a]						
dihedral angle	1	2	3	4A	4B	5	6
C1−C14−C13−C12	26.9	29.9	44.3	33.0	36.7	37.0	34.3
C2−C1−C14−C13	107.5	109.7	120.9	113.0	117.2	113.1	120.9
C7−C6−C5−O	119.1	109.3	112.5	111.4	112.0	114.3	112.5
C8−C9−C10−C11	55.6	55.5	57.7	58.6	58.8	63.6	57.5
C11−C12−C13−C14	34.1	34.8	45.4	39.4	41.0	42.1	45.4

[a] Compounds included: (1) 10-deacetyl baccatin III; (2) baccatin III; (3) Taxotere; (4A) Taxol, molecule A of asymmetric unit; (4B) Taxol, molecule B of asymmetric unit; (5) 2′-carbamate taxol; (6) 7-mesylpaclitaxel.

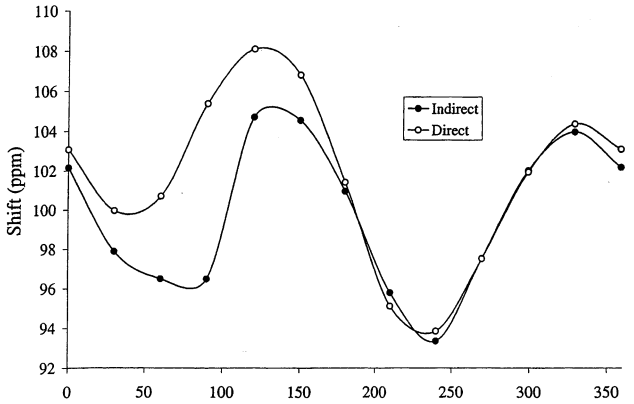

Figure 6. Tensor variation versus dihedral angle for the δ_{11} component of C4 in verbenol. Included are variations arising from OH rotation with and without additional structural refinements, the indirect and direct effects, respectively. Similar variations were observed for carbons 2, 3, and 5 and demonstrate that the direct effect accounts for only about half of the tensor differences observed.

FIREMAT ^{13}C data for polymorph I were collected on a 400 MHz Chemagnetics spectrometer operating at 100.62 MHz. The spectrum was acquired with TPPM ^{1}H decoupling[20] at a frequency of 400.12 MHz, a 180° pulse of 8.2 μs, and a 20° phase angle separating adjacent pulses. Spectral widths of 18.5 and 110.9 kHz were collected for the evolution and acquisition dimensions, respectively. A ^{1}H 90° pulse width of 4.1 μs was used together with a ^{13}C 180° pulse of 7.8 μs. A total of 32 evolution increments of 1152 scans each were collected with a 3 s recycle time for a total experiment time of 1.3 days. Evolution dimension data were extended to 9216 points using the previously described replication scheme inherent in the FIREMAT approach.[8] Digital resolutions of 12.03 Hz per point were obtained in both dimensions after the replication. A spinning speed of 578 Hz was used, and the spectrum was externally referenced to the high-frequency peak of adamantane at 38.56 ppm. Tensor values in all FIREMAT analyses were obtained using previously described procedures and software.[8,21]

A FIREMAT analysis of polymorph II was performed using the above parameters with the following variations. Spectral widths of 20.8 and 124.8 kHz were acquired for the evolution and acquisitions dimensions, respectively. Data were collected for only 576 scans per increment, decreasing total analysis time to 15.4 h. After data replication, digital resolutions of 20.3 Hz per point were obtained for both dimensions. Analysis was performed at a spinning speed of 650 Hz.

Low-temperature solid-state NMR data for polymorph I were collected on a Varian VXR 200 MHz horizontal bore instrument operating at 50.32 MHz. Isotropic spectra were collected at 23, −100, and −120 °C using a Doty 7.0 mm HS probe and spinning speeds of 4, 4, and 3 kHz for the respective temperatures. All reported temperatures were uncalibrated. All spectra were acquired with cross-polarization, a 33.0 kHz spectral width, a 3.1 s recycle time, and a 4.0 μs ^{13}C 90° pulse width and referenced to the methyl peak of hexamethyl benzene at 17.35 ppm. A digital resolution of 8.2 Hz per point was achieved for all spectra.

INADEQUATE analysis was performed using a Varian INOVA 500 MHz spectrometer operating at 125.76 MHz. Data were acquired using a 141 mg sample of 10-deacetyl baccatin III dissolved in 0.7 mL of d_6-DMSO. Spectral widths of 27.2 kHz were acquired for both dimensions. A total of 256 increments of 128 scans per increment were collected with a 6 s recycle time, giving a total analysis time of 4.6 days. Other analysis parameters include an analysis temperature of 26 °C, an input J_{CC} value of 55 Hz, and a ^{13}C 90° pulse of 11.5 μs. Digital resolutions of 106.3 and 0.25 Hz per point for the evolution and acquisition dimensions were acquired, respectively.

Tensors were computed using the B3LYP method and the D95** basis set for polymorph I. X-ray geometry was used for heavy atoms, while hydrogen positions were refined by the B3LYP method with the D95* basis set. Computed shielding values were correlated to shifts allowing shieldings to be converted to shifts using respective slope and intercept values of −1.04 and 186.74 for sp^3 carbons and −1.01 and 191.43 for sp^2 carbons. An overall root-mean-square (rms) error of 4.72 ppm was found for all computed tensors with errors of 7.06 and 3.43 ppm for sp^2 and sp^3 carbons, respectively.

Two tensor computations were performed for polymorph I that included DMSO molecules at the X-ray positions. These two structures are needed to mimic the thermal motion found for the DMSO at C1. The second DMSO at C7 was retained in the same position in both calculations. The final tensors were obtained by averaging the two sets of individual tensors for each molecular structure, thereby simulating the 50/50 occupancy suggested by X-ray analysis.

Tensors for polymorph II were computed at the B3LYP/D95** level of theory. The molecular geometry used consisted of an energy-minimized structure obtained from the B3LYP method and the D95 basis set. Computed shieldings were converted to shifts using respective slope and intercept values of −1.11 and 186.22 for sp^3 carbons and −1.02 and 186.57 for sp^2 carbons. An overall rms error of 6.46 ppm was observed in computed tensors with errors of 10.47 and 3.94 ppm for sp^2 and sp^3 carbons, respectively.

Acknowledgment. Computer resources for tensor computations were provided by the Center for High Performance Computing at the University of Utah. This work was supported by the National Institutes of Health under Grant GM08521-40 to D.M.G. We thank Dr. F. G. West and Bristol-Myers Squibb for donation of the 10-deacetyl baccatin III sample used and Dr. Anita M. Orendt for collection of all low-temperature isotropic spectra.

JA020371A

(20) Bennett, A. E.; Reinstra, C. M.; Auger, M.; Lakshmi, K. V.; Griffin, R. J. *J. Chem. Phys.* **1995**, *103*, 6951.
(21) Sethi, N. K.; Alderman, D. W.; Grant, D. M. *Mol. Phys.* **1990**, *71*, 217.